Volume 1, Number 4 (December, 2008) p. 331 - 364 • ISSN 1983-4195

REVISTA IBRACON DE ESTRUTURAS E MATERIAIS

IBRACON STRUCTURES AND MATERIALS JOURNAL

Flexural Analysis of Prestressed Concrete Structures

Modelos de Verificação à Flexão de Estruturas Protendidas

M. B. CAVALCANTI [a]
marlonbc@ibest.com.br

B. HOROWITZ [b]
horowitz@ufpe.br

Abstract

In the computation of the strength capacity of prestressed concrete structures prestressing may be viewed as strength or load. “Model 1” considers prestressing strands as integral part of the cross section where prestressing operation induces imposed deformations corresponding to prestraining. Alternatively, “Model 2” considers prestressing as external loading, composed of a self-equilibrating system of forces on the anchorages and transversely on concrete. After transfer prestressing strands are considered as conventional reinforcement in computations except that the deformation axis is displaced to take into account pre-elongation. In spite of Model 1 being the most commonly used in designing of continuous beams and officially adopted by NBR 6118 it has the inconvenience of the mandatory consideration of additional secondary effects known as hyperstatic moments which must be taken into account in ultimate strength analysis. The computation of secondary effects is simple for continuous beams but becomes more involved in cases of frames and grids and infeasible in cases of plates and shells. In Model 2 there is no need to compute secondary effects but the cross section must be verified for combined axial force and bending moment. In order to compare results from the models two examples are presented: one example of a statically indeterminate frame and finally an example of a prestressed bridge deck is presented using grillage analogy.

Keywords: Prestress, Continuous, Secondary Effects.

Resumo

No cálculo da capacidade portante de estruturas protendidas a protensão pode ser considerada tanto como resistência quanto como carga. Tem-se, portanto, o “Modelo 1” que considera os cabos como parte integrante da seção, onde a operação de protensão induz deformação imposta correspondente ao pré-alongamento das armaduras ativas. Alternativamente, tem-se o “Modelo 2” que considera a protensão como caso de carregamento externo, composto por sistema auto-equilibrante de forças nas ancoragens e transversais no concreto. Após ativação da aderência os cabos de protensão são considerados no cálculo como armadura convencional, apenas deslocando o eixo das deformações para levar em conta o pré-alongamento. Apesar do “Modelo 1” ser mais utilizado no dimensionamento de vigas contínuas e estar consagrado na NBR-6118, ele possui o inconveniente do surgimento de esforços adicionais denominados efeitos hiperestáticos de protensão, que precisam ser considerados na verificação a ruptura. O cálculo dos efeitos hiperestáticos de protensão é relativamente simples no caso de vigas contínuas, porém torna-se complexo no caso de pórticos e grelhas e inviável no caso de lajes e cascas. Já no “Modelo 2” não há necessidade do cálculo dos efeitos hiperestáticos, porém as seções forçosamente terão que ser verificadas à flexão composta. Para comparar os resultados dos modelos são apresentados dois exemplos: um pórtico e uma de laje de tabuleiro de viaduto analisado utilizando-se analogia de grelha.

Palavras-chave: Protensão, Continuidade, Hiperestáticos.

[a] *Departamento de Engenharia Civil, Universidade Federal de Pernambuco, marlonbc@ibest.com.br, Av. Acadêmico Hélio Ramos, s/n, 50740-530, Recife – PE – Brasil;*

[b] *Departamento de Engenharia Civil, Universidade Federal de Pernambuco, horowitz@ufpe.br, Av. Acadêmico Hélio Ramos, s/n, 50740-530, Recife – PE – Brasil.*

1. Introduction

1.1 Description of the problem

Provisions of international codes for verification of prestressed concrete members fall into two types of models where prestressing can be considered as imposed deformation corresponding to pre-elongation of active reinforcement, or as external loads comprised of a self-equilibrating system of equivalent loads.

Prestressing considered as imposed deformations induces in statically indeterminate structures the occurrence of secondary effects, due to deformation restraint, and that must be taken into account in ultimate strength checks.

Prestressing considered as external loading consists of a self-equilibrating forces on the anchorages and transverse distributed forces on the concrete. After bonding prestressing strands can be considered as conventional passive reinforcement except that pre-elongation must be taken into account.

European codes allow adoption of both models for consideration of prestressing. Brazilian as well as American codes although not explicitly enforcing either model, adopt implicitly the imposed deformation model since they require consideration of secondary effects in ultimate strength verifications.

The verification of prestressed members in international codes is based on representative values of the prestressing force. The design value of the prestressing force is given by its representative value multiplied by the corresponding factor.

1.2 Objectives

The main objective of this work is to exemplify a methodology where the calculation of secondary effects of the prestressing is not necessary. It is also the aim of this study to compare results obtained with the usual methodology that considers prestressing as resistance, since modern design codes make use the dual vision of prestressing either as resistance, or as load, they should produce the same results, thus contributing the discussion of the appropriate value of γ_p in the Brazilian code.

Figure 1 – Diagram tension-deformation used in model 2

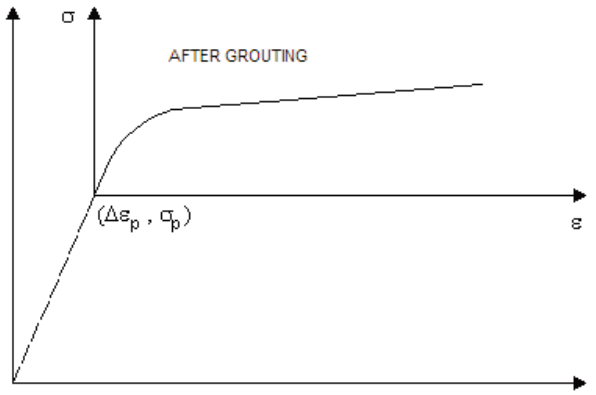

2. Prestressing as external loading

2.1 Models of calculation

The effects of the prestressing can be considered either as action or resistance caused by pre-elongation (section 5.10.1 of the EC2 [1]). Thus two possible verification models may be considered, namely:

- **Model 1:** Considers the prestressing strands as integral part of the cross section, where prestressing operation introduces imposed deformation corresponding the pre-elongation of the active reinforcement.
- **Model 2:** Considers prestressing as external loading consisting of a self-equilibrating system of forces in the anchorages and the transversally in the concrete. After transfer prestressing strands are considered as conventional reinforcement, only taking into consideration the pre-elongation.

2.2 Prestressing considered as external action

In this model the structure is considered to be acted upon by external forces computed as equivalent prestressing loads, where prestressing steel after grouting is considered as conventional passive reinforcement, only with the origin of its stress/strain curve shifted by the pre-elongation $(\Delta\varepsilon_p)$ and corresponding stress (σ_p) (see Figure [1]).

In the analysis of statically indeterminate structures with prestressing considered as external loading, there is no need to compute secondary effects. This simplifies the verification, since the total prestressing effects can be directly obtained from the output of the analysis program.

3. Verification of prestressed concrete sections

3.1 Introduction

The European codes allow the use of both models of verification mentioned above. Both NBR 6118 [2] and ACI 318-02 [3] do not make direct comments on the models of verification, however as they use the concept of "secondary effects" of prestressing they implicitly adopt model 1.

Both EC2 and NBR 6118 indicate three representative values for the prestressing force: medium, P_m, characteristic upper/lower, $P_{k\,\mathrm{sup}}$ e $P_{k\,\mathrm{inf}}$. ACI considers only the mean value only. Except for NBR 6118, all other codes unanimously specify P_m as the value to be used in the verifications of resistant capacity. NBR 6118 makes exceptions in section 9.6.1.3 when the losses exceed 35% and in the case of "special structures".

The design value for the prestressing force is given by the expression:

$$P = \gamma_p \, P_k \qquad (3.1)$$

where, γ_p = load factor for prestressing; P_k = representative value of prestressing force at a given section in a given time.

All codes except NBR 6118 specify $\gamma_p = 1$ for global verifications. In fact, in section 11.7.1 of NBR 6118 it is specified $\gamma_p = 0{,}9$

Figure 2 – Domains of the ultimate limit state – ELU (NBR 6118)

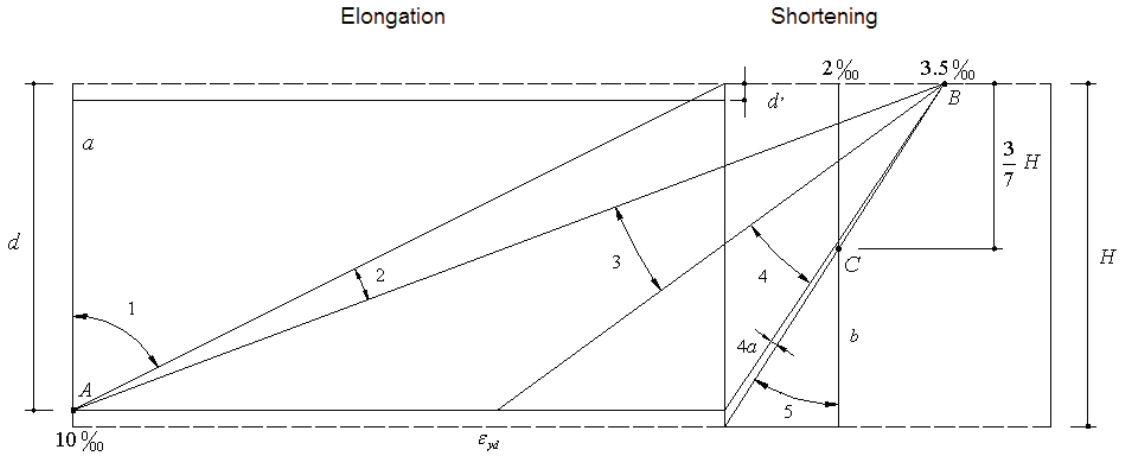

for favorable effects and $\gamma_p = 1{,}2$ unfavorable effects. EC2 in the section 2.4.2.2 specifies $\gamma_p = 1$ for favorable actions and $\gamma_p = 1{,}3$ or $1{,}2$ for unfavorable actions, in the cases of external prestressing and local verifications, respectively.

As prestressing is in the vast majority of the times a favorable effect in the case of the resistant capacity in bending, and adopting $\gamma_p = 0.9$, the results of the two models mentioned above will only coincide if the pre-elongation and the equivalent prestressing loads are computed on the basis of the same design value of the prestressing force.

3.2 Characterization of the ultimate limit state according to NBR 6118

The ultimate limit state is characterized when the distribution of the deformations in the cross section to belong to one of the domains defined in Figure [2].

The deformations of extreme fibers corresponding to an ultimate limit state can be conveniently expressed as a function of a single dimensionless parameter, D [4]. It is presented below a slightly modified procedure from Ref.[4] in order to include the domain 4a. The deformation corresponding to the compressed concrete fiber, $\varepsilon_s(D)$, and the corresponding deformation of the most tensioned steel, $\varepsilon_i(D)$, can be seen in the Table [1], where the relationship is presented between domains 1 the 5 (for positive moment) and 5 ' the 1 ' (for negative moment) with the values of D.

In Table [1]: y_s = distance of the compressed extreme fiber to the CG of the section; y_i = distance of the tension extreme

Table 1 – Correspondence between the domains of ELU and D

Dom.	D	y_s	$\varepsilon_s(D)$‰	y_i	$\varepsilon_i(D)$‰
1	$0 \le D < 2$	y_{sup}	10 - 5 D	y_{min}	10
2	$2 \le D < 7$	y_{sup}	1,4 - 0,7 D	y_{min}	10
3/4	$7 \le D \le 12$	y_{sup}	-3,5	y_{min}	24 - 2D
4a	$12 < D < 13$	y_{sup}	-3,5	y_{min}	$12\varepsilon_{4a} - \varepsilon_{4a}D$
5	$13 \le D < 14$	y_{sup}	-23 + 1,5 D	y_{inf}	26 - 2D
5'	$14 \le D \le 15$	y_{sup}	-30 + 2 D	y_{inf}	19 - 1,5D
4a'	$15 < D < 16$	y_{max}	$-16\varepsilon_{4a'} + \varepsilon_{4a'}D$	y_{inf}	-3,5
3'/4'	$16 \le D < 21$	y_{max}	-32 + 2D	y_{inf}	-3,5
2'	$21 \le D < 26$	y_{max}	10	y_{inf}	-18,2 + 0,7D
1'	$26 \le D \le 28$	y_{max}	10	y_{inf}	-130 + 5D

Figure 3 – Illustration of the described variable in Tab. 3.1

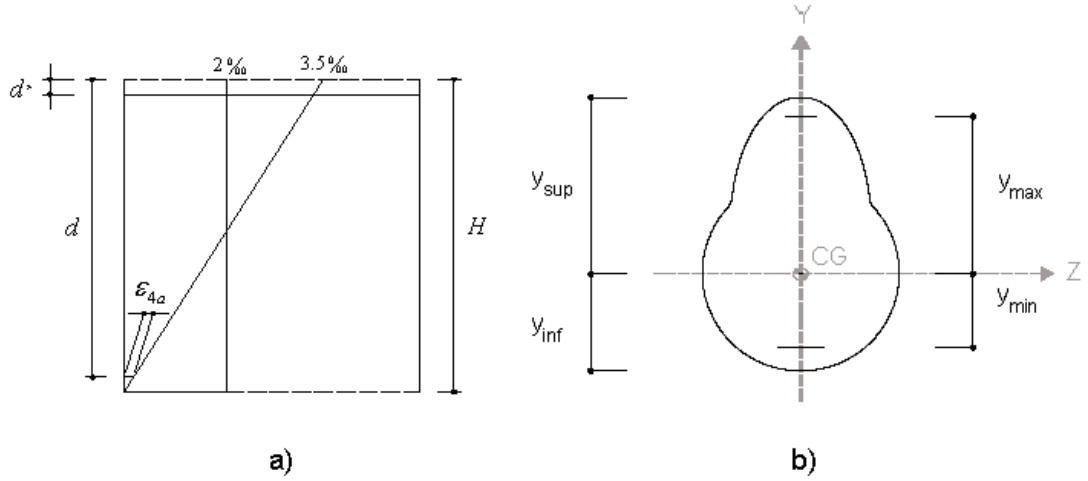

fiber to the CG of the section. Still for Table [1] one has that:

$$\varepsilon_{4a} = \frac{3,5}{H}\left(y_{inf} - y_{min}\right);\ \varepsilon_{4a}' = \frac{3,5}{H}\left(y_{sup} - y_{max}\right) \quad (3.2)$$

where ε_{4a} (and consequently ε_{4a}') corresponds to the segment indicated in the Figure [3 a]. The remaining variables can be seen in the Figure [3 b].

In Figure [3 b] one has that: y_{max} = distance of the uppermost reinforcement to the CG of the section; y_{min} = distance of the lowest reinforcement to the CG of the section.

3.3 Procedures for the verification of prestressed sections

At this stage it is presented a description of the logical sequence of

Figure 4 – Flowchart of routines 1 and 2

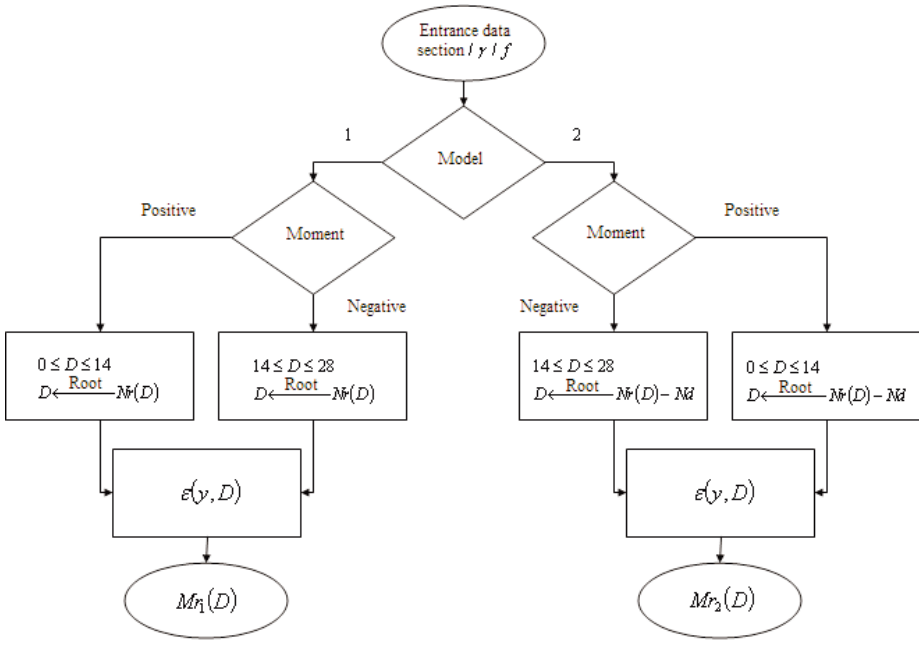

the computation procedures developed for the software Mathcad 2000 Professional [5], according to the flowchart shown in Figure [4], which describes the main steps for verification of sections.

3.3.1 Routine 1 – computation of the ultimate design moment for model 1

Initially the defining data of the concrete section, the layers of reinforcement and load and resistance factors are requested. Once the input data becomes available it is initiated the analysis of the section aiming at obtaining the deformation profile at the ultimate limit state. The following main steps are executed: processing of the constitutive relationships for concrete and steel as well as of the axial force corresponding to the section deformations, as given by the following expression:

$$Nr(D) = \int_{y_{inf}}^{y_{sup}} b(y)\,\sigma_{cd}(\varepsilon(y,D))\,dy + \sum_{cam\ s} A_s\,\sigma_{sd}(\varepsilon(y,D)) + \sum_{cam\ p} A_p\,\sigma_{pd}(\varepsilon(y,D)) \quad (3.3)$$

where, Nr = resisting axial force; $b(y)$ = width of the section at ordinate y ; cam s, cam p = layers of passive and active reinforcement in the section.
The deformation profile corresponding to the ultimate limit state is found solving the equation:

$$Nr(D) = 0 \quad (3.4)$$

Once the value of D is known the resisting bending moment, Mr , can be computed by the expression:

$$Mr(D) = \int_{y_{inf}}^{y_{sup}} b(y)\,\sigma_{cd}(\varepsilon(y,D))\,y\,dy + \sum_{cam\ s} A_s\,\sigma_{sd}(\varepsilon(y,D))\,y_s + \sum_{cam\ p} A_p\,\sigma_{pd}(\varepsilon(y,D))\,y_p \quad (3.5)$$

3.3.2 Routine 2 – computation of the ultimate design moment for model 2

In this routine the data defining to the concrete section, the layers of reinforcement and load and resistance factors are also initially requested. As distinguishing feature from the previous routine the definition of the constitutive relationship for the prestressing steel has its origin displaced to the point $(\Delta\varepsilon_p, \sigma_p)$. The remaining constitutive relationships do not change. The deformation profile of the section in the ultimate limit state is found solving the equation:

$$Nr(D) - Nd = 0 \quad (3.6)$$

where Nd corresponds to the acting axial force in the section and is computed by the expression:

$$Nd = Np + \gamma_f\ Nq \quad (3.7)$$

where, Np = design value of the axial force due to prestressing (negative for compression); γ_f = load factor for external acting forces; Nq = value of the additional axial force. With the known value of D, Mr is computed according to the expression (3.5).
Because of the differences in the consideration of the prestressing between the two models, the ultimate resisting bending moments are related according to:

$$Mr_2(D) = Mr_1(D) - Nd\ e \quad (3.8)$$

where, e = eccentricity of the average prestressing strand in relation to the CG of the section.

4. Examples of prestressed structures

4.1 Introduction

In this section two examples of statically indeterminate prestressed structures are presented: a plane frame and a bridge deck. The structures will be verified by the two models of consideration of the prestressing. The objective is to demonstrate the equivalence of the models in the calculation of the resistant capacity of prestressed structures.

4.2 Example of a statically indeterminate frame

Consider the prestressed statically indeterminate frame shown in the Figure [5], where the layout of the prestressing strand is divided in four concordant parabolic parts, as shown for half span of the beam. The objective is to determine the value of the uniform load, q_u , acting throughout the beam,so that the frame reaches the ultimate limit state of bending. The effective prestressing force is $P = 3{,}6$ MN and in order to simplify the discussion of the problem the following simplifications are adopted: P it is the effective force of prestressing in the considered age and constant throughout the prestressing strand, the prestressing steel as well as regular steel are considered elastic-plastic with yield limit f_{py} and f_{sy} , the reinforcement yields in the ultimate limit states, the load and resistance factors are taken equal to one, the rectangular stress diagram is adopted for the concrete and the neutral axis is assumed to fall inside the top flange.
Initially the frame is verified according to model 1 as indicated in the Figure [6 a], where a = depth of the compression block in the concrete with constant stress of $0.85\,f_{ck}$; F_c = resultant of the compression stresses in the concrete; F_p = resultant of the tensile stresses in the prestressing steel; M_u = ultimate resisting moment. After that, we will verify the frame for model 2 as indicated in the-

Figure [6 b], where ΔF_p = resultant of the tensile stresses in the prestressing steel, considered as regular reinforcement, after grouting of prestressing strands.

4.2.1 Model 1

The elastic restraint offered by the columns of the frame causes induces external loads, called secondary effects of prestressing.

In the example frame secondary effects are: hyperstatic bending moment and hyperstatic axial force.

The hyperstatic axial force due to prestressing corresponds to the reaction of the frame columns to the axial deformation imposed on the beam from the prestressing, thus causing a tensile axial force in the member that results in a reduction of the effective prestressing force (see Figure [7]).

Figure 5 – Prestressed frame

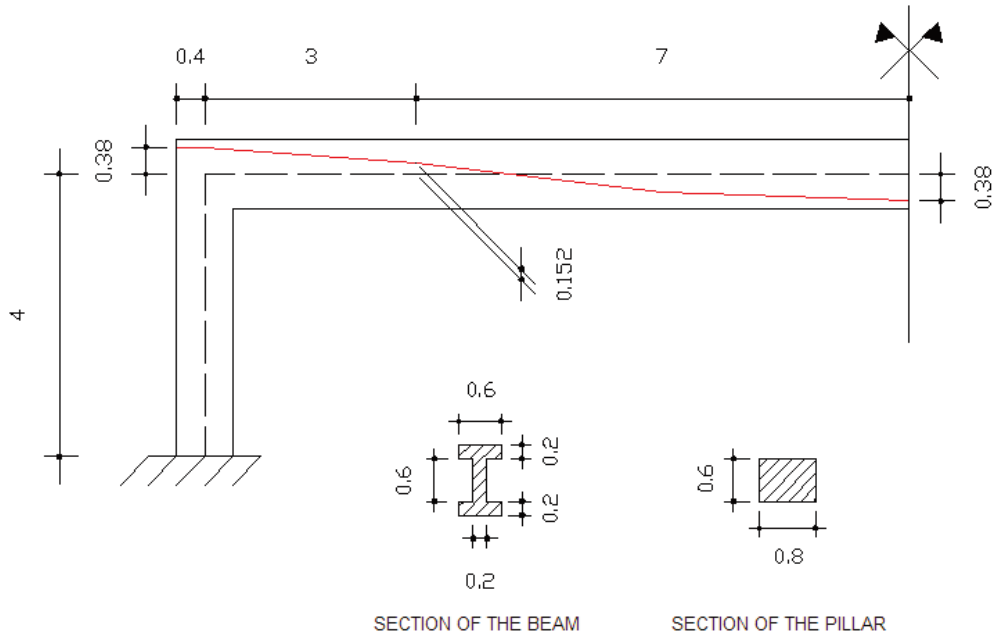

Figure 6 – Diagrams tension-deformation; a) model 1; b) model 2

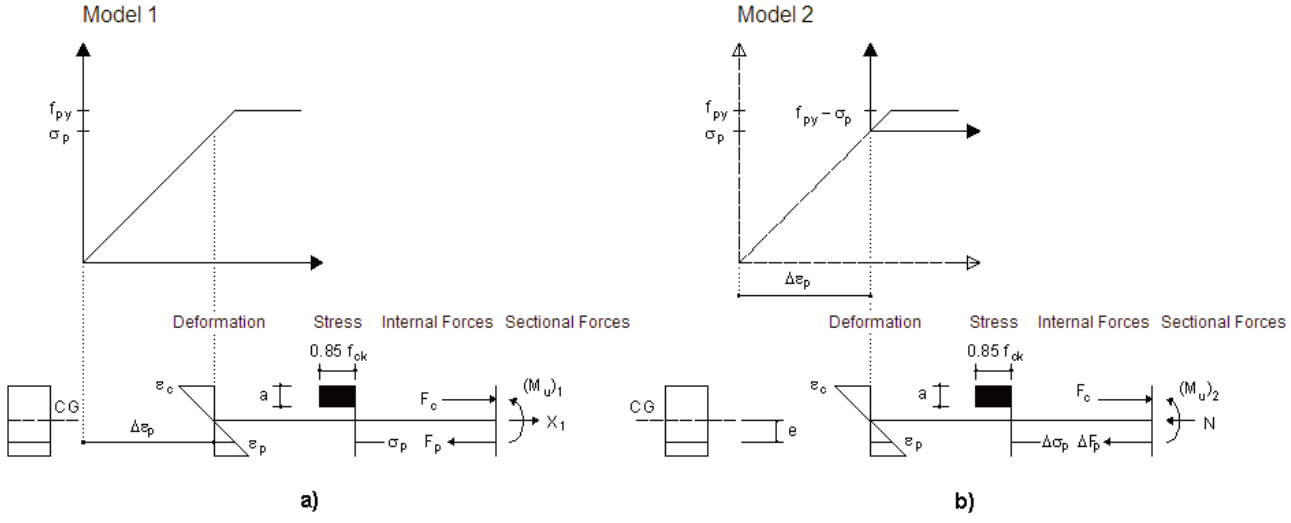

Figure 7 – Prestressed frame and secondary effects of the prestressing in the imposed deformation

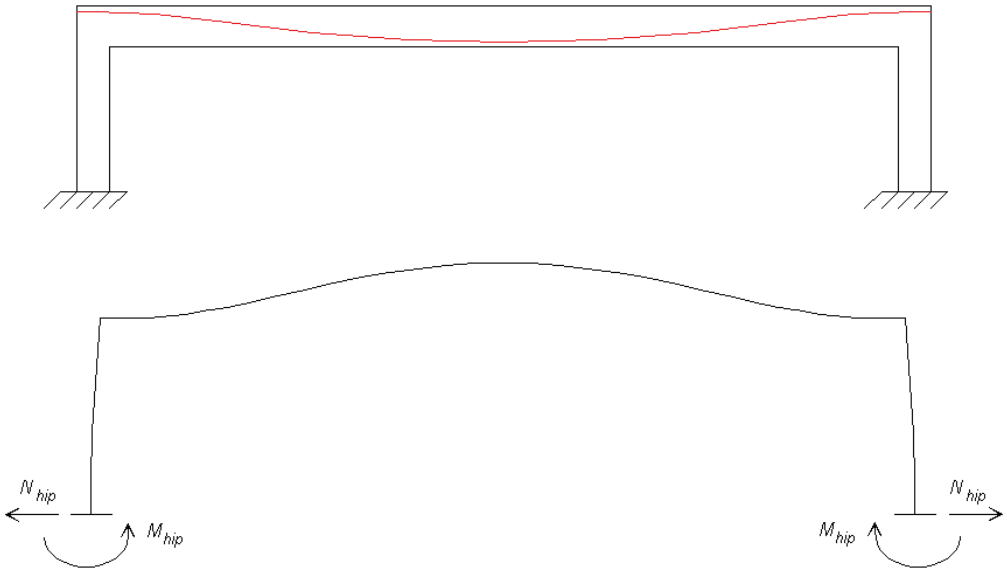

Figure 8 – Illustration of the method of flexibility

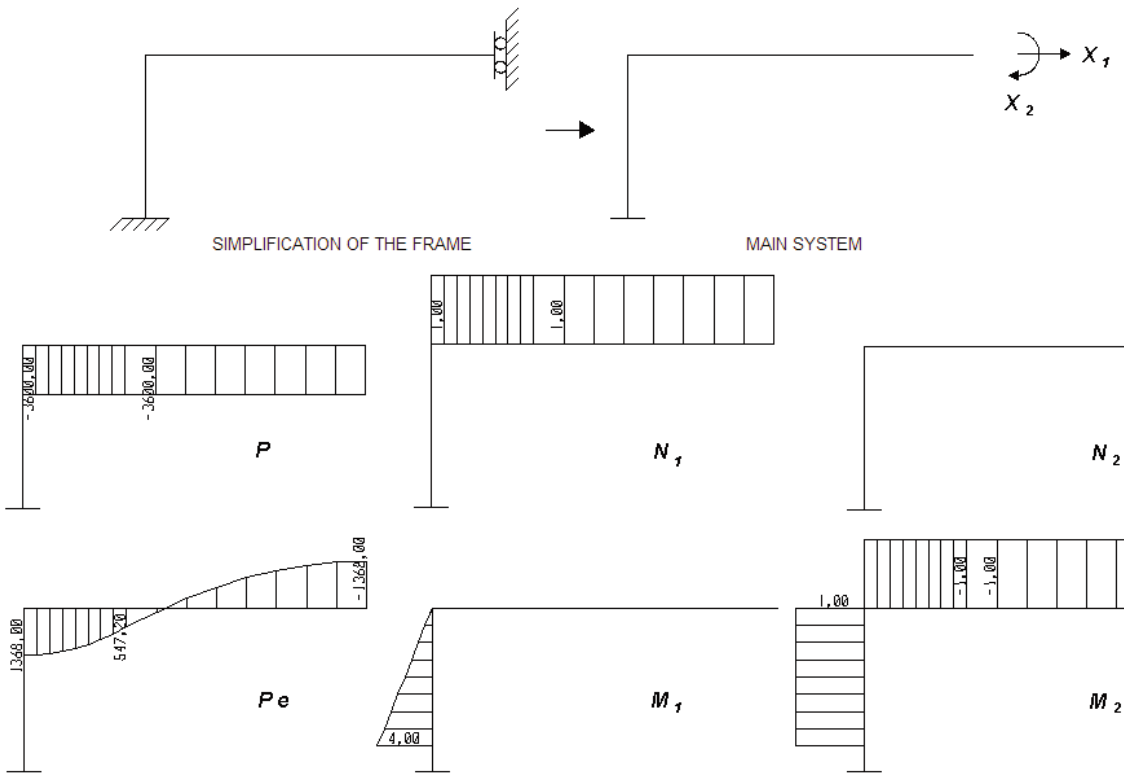

For each verified cross section the calculation procedure is:
– Compute the ultimate resisting bending moment, M_u .
– Compute the acting bending moment due to a unit external loading, M_{q1} .
– Equating the resistant and acting moments the value of q_u corresponding to the ultimate limit state can be solved for.

In the model 1 the acting moment in any given to section is:

$$M_{su} = q_u \; M_{q1} + X_2 \qquad (4.1)$$

where, X_2 = hyperstatic bending moment.

One can simplify the frame as in the Figure [8], where to each of the fixed displacements corresponds a support reaction, in this case, a force reaction and a moment reaction.

The equations that impose the conditions of compatibility of the Figure [8] can be written as:

$$\begin{bmatrix} \delta_{11} & \delta_{12} \\ \delta_{21} & \delta_{22} \end{bmatrix} \begin{Bmatrix} X_1 \\ X_2 \end{Bmatrix} + \begin{Bmatrix} \delta_{01} \\ \delta_{02} \end{Bmatrix} = \begin{Bmatrix} 0 \\ 0 \end{Bmatrix} \qquad (4.2)$$

where δ_{11}, δ_{12}, δ_{21}, δ_{22}, correspond flexibilities due to application of unit loads and unit moment; δ_{01} and δ_{02} correspond the imposed deformations on the structure due to prestressing. Applying the principle of the virtual work, one has:

$$\delta_{11} = N_1 \left(\frac{N_1}{E_c \; A_v} \right) L_v + \int_0^4 M_1 \left(\frac{M_1}{E_c \; I_p} \right) dx \qquad (4.3)$$

$$\delta_{22} = \int_0^{10} M_2 \left(\frac{M_2}{E_c \; I_v} \right) dx + \int_0^4 M_2 \left(\frac{M_2}{E_c \; I_p} \right) dx \qquad (4.4)$$

$$\delta_{01} = N_1 \left(\frac{-P}{E_c \; A_v} \right) L_v \; ; \; \delta_{02} = \int_0^{10} M_2 \left(\frac{P \; e}{E_c \; I_v} \right) dx \qquad (4.5)$$

where, A_v = cross sectional area of the beam; I_p = moment of

Figure 9 – Prestressing as external loading; a) the loads; b) diagrams and reactions

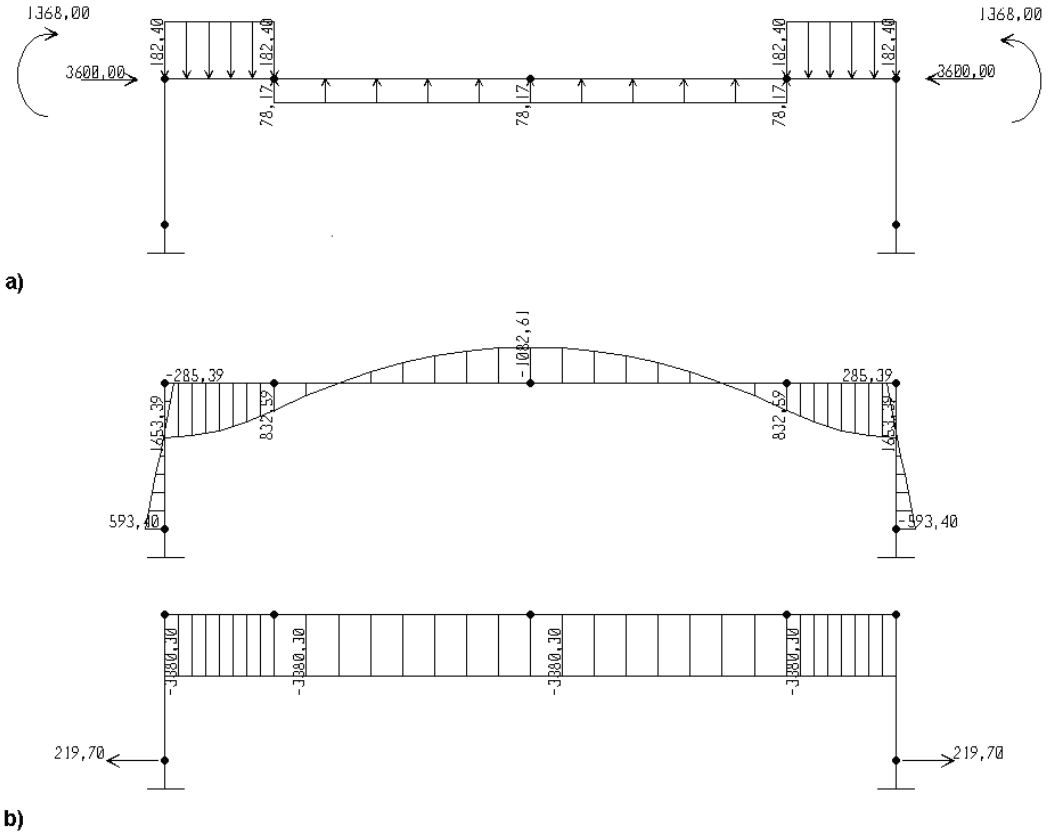

inertia of the columns; I_v = moment of inertia of the beam; L_v = length of the considered portion of the beam.

Solving the system for the example data one gets: $X_1 = 219{,}7$ kN e $X_2 = -285{,}39$ kN-m, which correspond to the secondary

Table 2 – Numerical data for the example of the frame

Data of the concrete and the steel			
f_{ck} = 50	MPa	E_p = 195000	MPa
E_c = 39597,98	MPa	Δ_{ep} = 7,385	‰
f_{py} = 1900	MPa	A_p = 2,5´10-3	m^2
Model 1		**Model 2**	
$(M_u)_1$ = 3,668	MN-m	$(M_u)_2$ = 2,3	MN-m
$(q_u)_1$ = 0,155	MN/m	$(q_u)_2$ = 0,155	MN/m

Figure 10 – Span of the prestressed hyperstatic plate

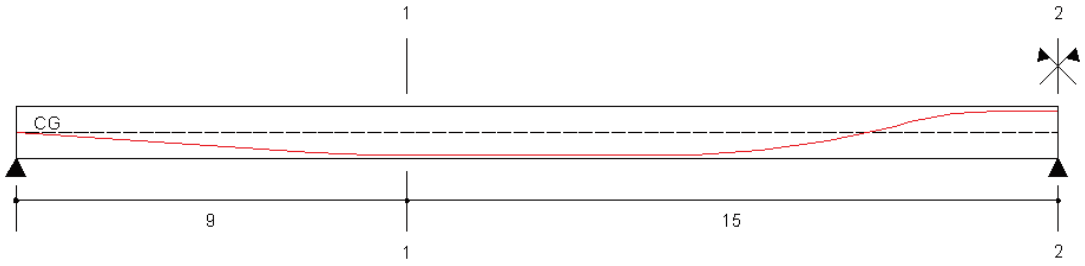

Figure 11 – Transversal section of the plate

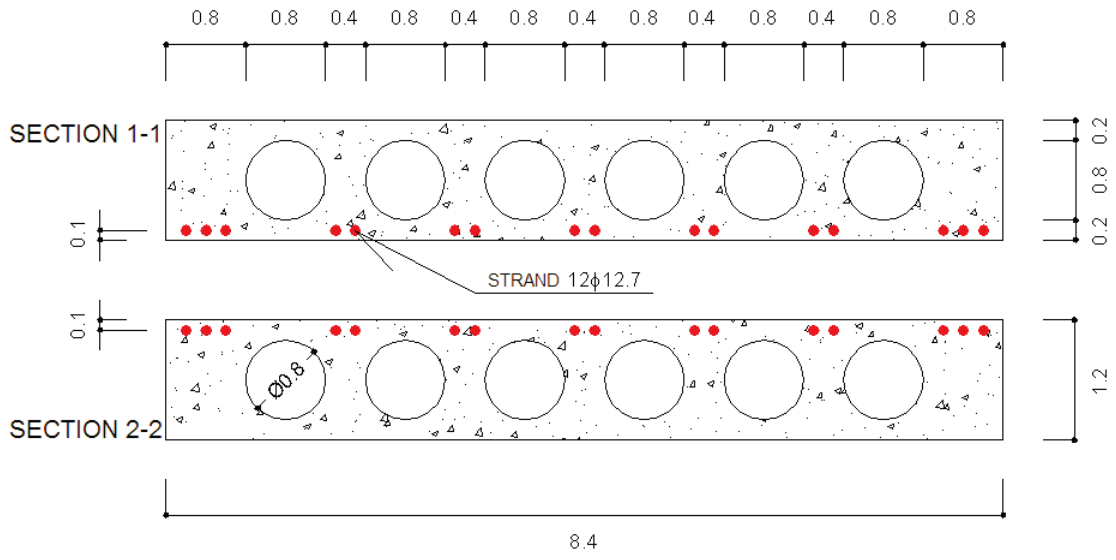

effects of prestressing. For each section q_u is given by:

$$(q_u)_1 = \frac{(M_u)_1 + X_2}{M_{q1}} \quad (4.6)$$

4.2.2 Model 2

The procedure for computation of the resisting moment is similar to the one of model 1. However, the sections in this model are submitted to the axial force due to prestressing.
The value of the acting bending moment in the considered section is:

$$M_{su} = q_u \, M_{q1} + M_{qp} \quad (4.7)$$

where, M_{qp} = bending moment due to prestressing only.
The ultimate load in the section under study is equal to:

$$(q_u)_2 = \frac{(M_u)_2 - M_{qp}}{M_{q1}} \quad (4.8)$$

In Figure [9 a] shows prestressing as external loading and, in the Figure [9 b] shows the bending moment diagram of due to this loading as well as the axial force diagram and the reactions exerted in the supports, where the units are kN and m.
Table [2] presents values for the concrete and steel, as well as the obtained results. As can be observed from the last line the final values of the load are identical for the two models of analysis.

4.3 Example of a statically indeterminate bridge deck

For the case of a slab loaded transversally, the verification of the ultimate limit state in bending, as in the case of frames, involves a problem of combined effects of axial force and bending moment, for both models, due to the hyperstatic axial force and prestressing.
Consider the prestressed bridge deck shown in the Figures [10, 11], where the layout of the prestressing strands is defined by the coordinates of Table [3]. The objective is to determine the intensity of the maximum moving load expressed through load factor λ, so that the first section reaches the ultimate limit state of bending. The average effective prestressing force of the 16 strands shown in the Figure [11], in each of the 16 segments, in which the span was subdivided, are also shown in the Table [3]. The cross section of the deck contains circular voids throughout the length, since no supports diaphragms were provided for simplicity.
The analysis of this problem follows the procedures of verification of the ultimate limit state of bending according to NBR 6118.
It is applied in this example the well known technique of grid analogy, that consists in modeling the deck as a set of grid members distributing the longitudinal and transversal stiffnes of the plate, respectively, in the longitudinal and transversal elements of the grid,

Table 3 – Coordinates and effective prestressing force in the segments of the span

Segments	Eccentricity of the strand (m)			Effective prestressing force (kN)		
	$e_{initial}$	e_{medium}	e_{final}	$P_{initial}$	P_{medium}	P_{final}
1	0,000	-0,050	-0,100	21055,3	21087,8	21120,3
2	-0,100	-0,150	-0,200	21120,3	21150,7	21181,1
3	-0,200	-0,249	-0,299	21181,1	21193,5	21205,9
4	-0,299	-0,349	-0,399	21205,9	21193,1	21180,3
5	-0,399	-0,444	-0,488	21180,3	21192,7	21205,2
6	-0,488	-0,494	-0,500	21205,2	21303,5	21401,8
7	-0,500	-0,500	-0,500	21401,8	21443,7	21485,5
8	-0,500	-0,500	-0,500	21485,5	21494,9	21504,2
9	-0,500	-0,500	-0,500	21504,2	21488,0	21471,8
10	-0,500	-0,500	-0,500	21471,8	21455,3	21438,9
11	-0,500	-0,478	-0,456	21438,9	21537,9	21636,9
12	-0,456	-0,378	-0,300	21636,9	21550,0	21463,1
13	-0,300	-0,164	-0,028	21463,1	21296,7	21130,3
14	-0,028	0,155	0,338	21130,3	20719,6	20309,0
15	0,338	0,419	0,499	20309,0	20040,3	19771,5
16	0,499	0,500	0,500	19771,5	19889,2	20006,9

Figure 12 – Set of elements of used grid

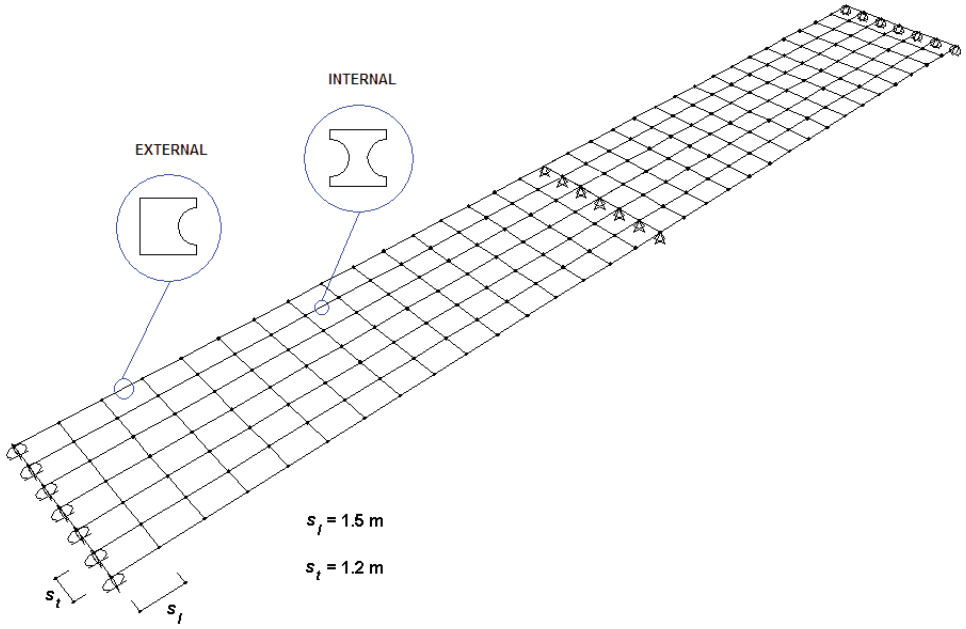

through the values of inertias in bending and twisting [6], as shown in the Figure [12]. The axes of the internal longitudinal members are located at mid distance between the centers of adjacent voids and the external members at half distance between the side of the deck and the center of the first void.

The deck is treated as an orthotropic plate and the properties of the longitudinal and transverse elements are determined separately [7]. The computation of moments of inertia of bending of the portions of longitudinal sections follows the classic methodology. In the determination of inertia of the transverse members it is recommended the usage of Elliott's Method, given by the expression below:

$$i = \frac{h^3}{12}\left[1 - 0{,}95\left(\frac{d_v}{h}\right)^4\right] \qquad (4.9)$$

where, i = moment of inertia for unit of width; d_v = diameter of the void.

Consequently, for the portions of transverse sections, the moment of inertia is given by:

$$I_t = s_l \cdot i \qquad (4.10)$$

where, I_t = moment of inertia of the transverse members; s_l = longitudinal width of the grid element.

For the inertia the twisting of voided plates per unit of height, it is recommended to use the Method of Ward and Cassell, where the torsional constants for the longitudinal and transverse members of the grid, respectively J_l and J_t, are given by:

$$j = 0{,}83\,\frac{h^3}{6} \qquad (4.11)$$

$$J_l = s_t\ j \qquad (4.12)$$

$$J_t = s_l\ j \qquad (4.13)$$

where, j = torsional constant for unit of width; s_t = width of the transverse grid members. Table [4] summarizes the geometric properties of the members.

4.3.1 Loading

The loading applied to nodes of the grid model consist of both distributed load multiplied by the influence area of each node and concentrated loads. The distributed loads consist of the own weight of the sections, pavement and traffic load. The concentrated loads model wheels loads.

Table 4 – Summary of the geometric properties

Properties of the sections					
External longitudinal		**Internal longitudinal**		**Transverse**	
A = 1,189	m^2	A = 0,937	m^2	A = 1,8	m^2
I = 0,163	m^4	I = 0,153	m^4	I = 0,175	m^4
J = 0,287	m^4	J = 0,287	m^4	J = 0,359	m^4

The value of distributed loads multiplied by influence area of each node are:
i) for own weight:

$$F_{ext} = A_{ext}\ b\ 25\ \text{kN/m}^3\ ;\ F_{\text{int}} = A_{\text{int}}\ b\ 25\ \text{kN/m}^3 \qquad (4.14)$$

ii) for pavement:

$$F_{ext} = \frac{a}{2}\ b\ esp\ 24\ \text{kN/m}^3\ ;\ F_{\text{int}} = a\ b\ esp\ 24\ \text{kN/m}^3 \qquad (4.15)$$

iii) for traffic loads:

$$F_{ext} = \frac{a}{2}\ b\ 5\ \text{kN/m}^2\ ;\ F_{\text{int}} = a\ b\ 5\ \text{kN/m}^2 \qquad (4.16)$$

where: , F_{ext} , F_{int} = concentrated loads in external and internal nodes due to distributed loading; , A_{ext} , A_{int} = cross sectional area of external and internal longitudinal members; a = height of the influence area; b = base of the influence area; esp = pavement thickness = 0,07 m.

Figure [13] shows influence areas of external and internal nodes. Figure [14] shows to the distributed load due to traffic and concentrated wheel loads of the vehicle class 45 on a region of the deck. Figure [14] also exemplifies the adopted treatment of moving loads on the plate.
The concentrated wheel loads coincide with nodes of the grid in the longitudinal direction for the adopted loading hypotheses. The same does not occur in the transverse direction, where redistribution loads becomes necessary. Table [5] summarizes the values of loads applied to grid nodes.

4.3.2 Loading hypotheses

In this case, only two sections are being analyzed of the longitudinal members, one in the external portion and one in the internal portion, of section 1-1 of Figures [10, 11].
In the determination of λ so that one of the two sections under study reaches the ultimate limit state of bending, two loading hypotheses are considered: hypothesis 1 and hypothesis 2.
In hypothesis 1 the loads of the central wheels of the vehicle are located in the first span, 15 m from the central supports, according to the influence line for bending moments in section 1-1 of the bridge deck. The remaining loads are applied to nodes of the first span only (see Figures [15, 16]).
In hypothesis 2 the loads of the central wheels of the vehicle are located in the first span, 10,5 m from the central support,

Figure 13 – Influence area of nodes

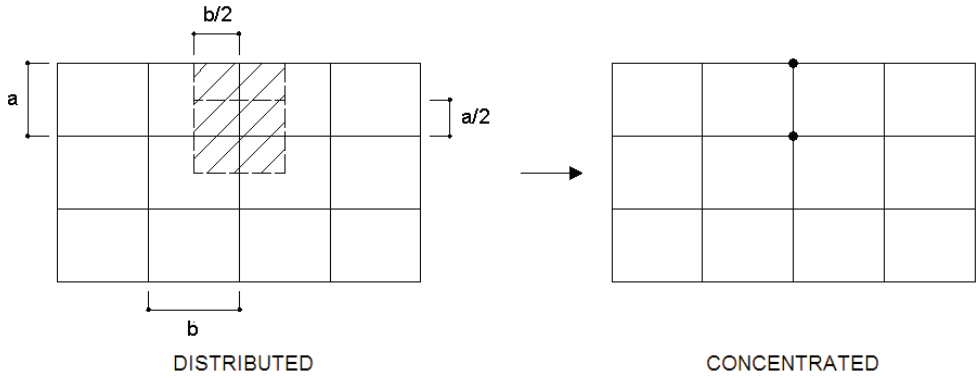

according to the influence line for bending moments in section 2-2 of the bridge deck. The remaining loads are applied to nodes of both spans.

4.3.3 Model 1

Using St Venant's principle and considering uniform the compression stresses due to prestressing, hyperstatic axial forces are obtained for the longitudinal members by multiplying this stress by the cross sectional areas of the members and deducting the isostatic value of the axial force due to prestressing. These hyperstatic axial forces result in tensile or compressive forces, depending on the portion of the effective prestressing force applied to each member of the analyzed

Figure 14 – Load due to traffic and loads of the vehicle

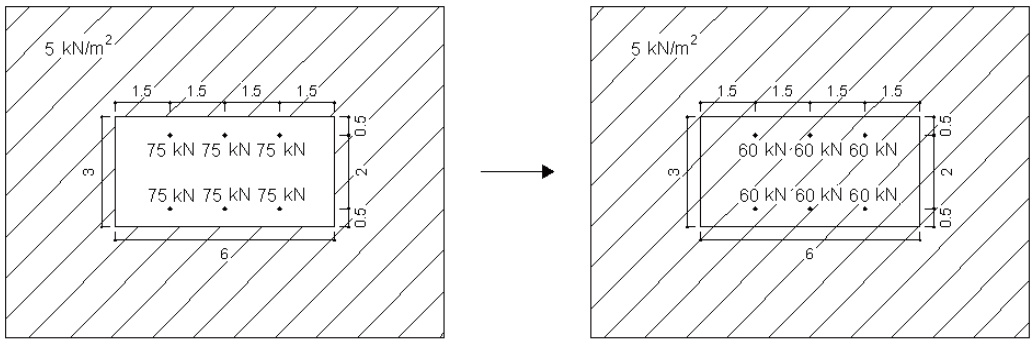

Table 5 – Summary of the values of loads applied to grid nodes

Loads (kN)	Sections	
	External Longitudinal	Internal Longitudinal
Own Weight	44,577	35,149
Pavement	1,512	3,024
Traffic loads	4,5	9
Vehicle	60	See Figure (16)

Figure 15 – Influence line for bending moments of the considered sections of the plate

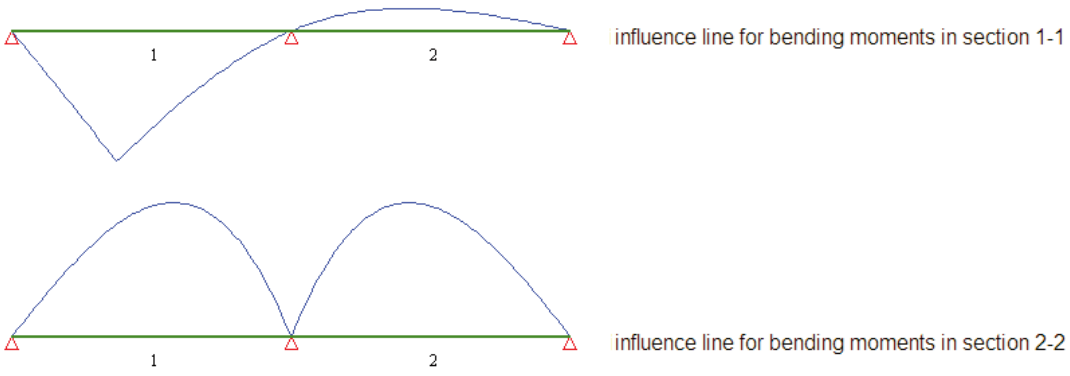

section. This procedure is described below, using the data from Table [3] and Figure [11].

$$(\sigma)_{1-1} = \frac{(P_{final})_{1-1}}{(A_{seção})_{1-1}} \quad (4.17)$$

$$(N_{tot})_{ext} = (\sigma)_{1-1}\ A_{ext}\ ;\ (N_{iso})_{ext} = \frac{3}{16}(P_{final})_{1-1} \quad (4.18)$$

$$(N_{tot})_{int} = (\sigma)_{1-1}\ A_{int}\ ;\ (N_{iso})_{int} = \frac{2}{16}(P_{final})_{1-1} \quad (4.19)$$

In both cases (internal and external):

$$N_{hip} = N_{tot} - N_{iso} \quad (4.20)$$

where, σ = compression stress in the considered section of the deck; P_{final} = effective prestressing force in the considered section of the deck; N_{tot}, N_{iso} and N_{hip} = axial forces due to prestressing in the section considered of the plate, respectively, total, isostatic and hyperstatic values. The Table [6] summarizes the values of axial forces.

For each member of deck section the calculation sequence is:

– Compute the ultimate resisting bending moment, $Mr(D)$.
– Get from commercial structural analysis programs the acting bending moments due to dead and moving loads, respectively, M_g and M_q.
– Equating the resisting and acting moments solve for λ, for which one of the members of the sections under study reaches the ultimate limit state.

Figure 16 – Loading hypothesis 1 of loads of the vehicle

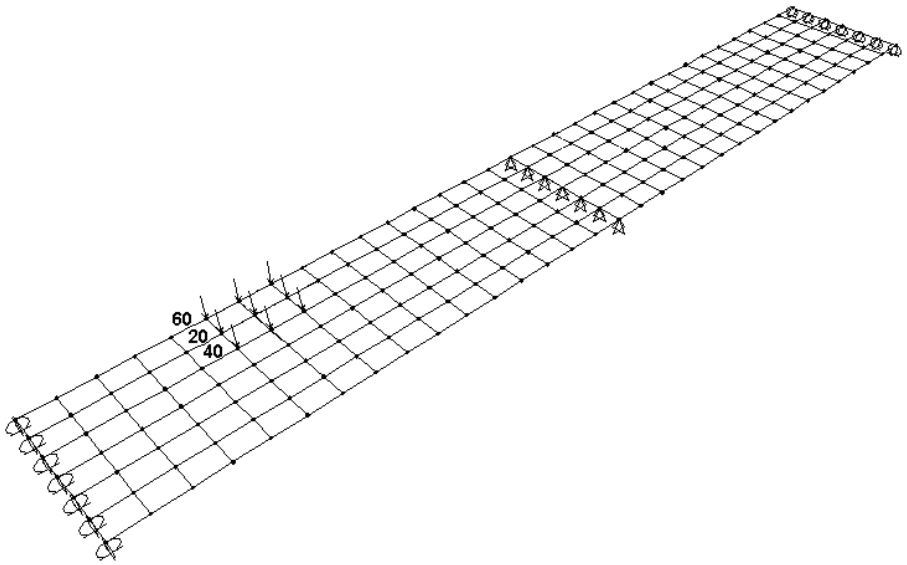

Table 6 – Summary of the values of the axial forces

Section 1-1		
Axial forces (MN)	**External**	**Internal**
N_{hip}	-0,412	0,164
N_{tot}	3,601	2,840

In the model 1 the acting moment in a given section is given by:

$$M_{su} = 1{,}35\, M_g + 1{,}5\, \lambda\, \varphi\, M_q + M_{hip} \quad (4.21)$$

$$\varphi = 1{,}4 - 0{,}007\, l = 1{,}232 \quad (4.22)$$

where, φ = impact factor for highway bridges; l = length, in meters, of each effective span of the loaded element, according to NBR 7187 [8].
The value of the hyperstatic prestressing moment can be obtained as follows:

$$M_{hip} = M_{qp} - M_{iso} \quad (4.23)$$

where, M_{iso} = isostatic prestressing moment; M_{hip} = hyperstatic prestressing moment. The total prestressing moment in the considered section is obtained from commercial structural analysis programs and the isostatic moment is given by:

$$M_{iso} = N_{iso}\, e \quad (4.24)$$

The values, in MN-m, of the ultimate resisting moments, acting moments as a function of dead and moving external loading, hyperstatics moments due the prestressing and factor λ, in the external and internal members of section 1-1 in loading hypotheses 1 and 2, are shown in Table [7], while Figure [17] illustrates the computation of the ultimate resisting moment for the internal members of section 1-1, through calculation routine 1.
In the result of the analyses of grid analogy there are discontinuities in bending moment diagrams in the two directions for loads applied to nodes, resulting from external loading multiplied by the area of influence of each node. For the values of bending moments, in each node, it was adopted the average of the two incident bars in each node.

4.3.4 Model 2

Similarly to model 1, in model 2 the acting moment in a given to-section is given by:

$$M_{su} = 1{,}35\, M_g + 1{,}5\, \lambda\, \varphi\, M_q + M_{qp} \quad (4.25)$$

Table [8] shows the moments and λ factors for model 2. Figure [18] is a sequel to Figure [17].
As the verification of the ultimate limit state of bending involves in both models combined action of axial force and bending moment, due to the hyperstatic axial force and prestressing, the calculation routines are modified as shown in Figures [17, 18].

5. Conclusions

From the discussion above, the main conclusions of this work are:

– For $\gamma_p \neq 1$, the results of the analysis of resistant capacity according to two models of consideration of the prestressing will only coincide if the pre-elongation and the equivalent prestressing loads are computed on the basis of the same design value of the prestressing force.
– NBR 6118 when emphasizing that the verification of the ultimate limit state must take into account the secondary effects of prestressing, implicitly endorses the use of model 1 in the prestressed concrete structures. It is desirable to contemplate model 2 also, since this would simplify the verification because load effects are directly obtained from the output of usual structural analysis programs.
– Due to equivalence of the two models the ambiguity in the consideration of the prestressing is commonly used, where the secondary effects of prestressing are extracted from the output of the analysis programs where prestressing is considered as external loading.

Table 7 – Summary of the values for model 1

Section 1-1					
Hypothesis 1	**Mr(D)**	**1,35 M_g**	**1,5 φ M_q**	**M_{hip}**	λ
External	5,154	2,058	1,089	0,682	2,22
Internal	3,753	1,931	0,983	0,093	1,76
Hypothesis 2	**Mr(D)**	**1,35 M_g**	**1,5 φ M_q**	**M_{hip}**	λ
External	5,154	1,546	0,729	0,682	4,02
Internal	3,753	1,451	0,678	0,093	3,26

Table 8 – Summary of the values for model 2

Section 1-1					
Hypothesis 1	**Mr(D)**	**1,35 M_g**	**1,5 φ M_q**	**M_{hip}**	**λ**
External	3,148	2,058	1,089	-1,325	2,22
Internal	2,415	1,931	0,983	-1,245	1,76
Hypothesis 2	**Mr(D)**	**1,35 M_g**	**1,5 φ M_q**	**M_{hip}**	**λ**
External	3,148	1,546	0,729	-1,325	4,02
Internal	2,415	1,451	0,678	-1,245	3,26

– The Brazilian code should consider the international trend of adopting $\gamma_p = 1$ for global verification of the resistant capacity of prestressed concrete structures with internal strands.

Figure 17 – Ultimate resisting moment for the internal members of section 1-1 for model 1

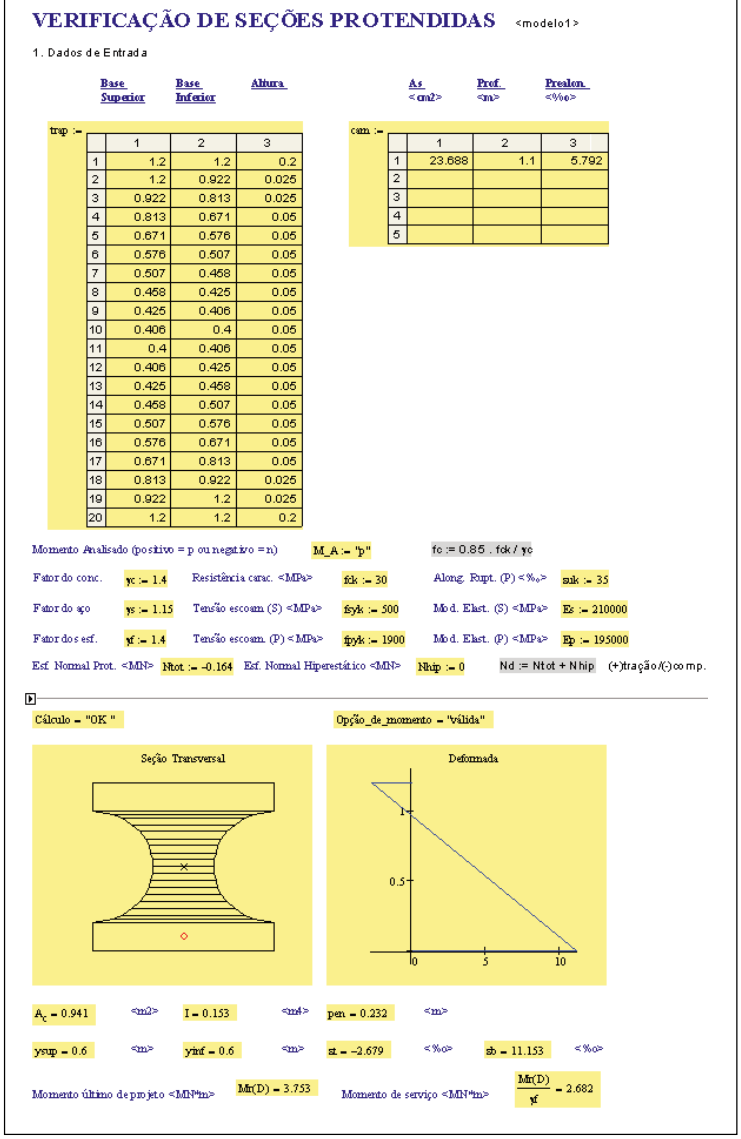

6. References

[01] EUROCODE 2 Ref. Nº EN 1992-1-1 (CEN, 2004), Design of Concrete Structures – Part 1.1: General Rules and Rules for Buildings, European Standard, English Version, April 2004.

[02] NBR 6118 – Março 2003 (ABNT, 2003), Projeto de Estruturas de Concreto – Procedimento, Associação Brasileira de Normas Técnicas, Rio de Janeiro, 2003.

[03] ACI 318-02, Building Code Requirements for Structural Concrete, American Concrete Institute, 2002.

[04] MUSSO Jr, F., "Dimensionamento de Seções de Concreto Armado e Verificação da Estabilidade de Vigas Colunas no Estado Limite", Dissertação de Mestrado, Pontifícia Universidade Católica do Rio de Janeiro, Depto. de Eng. Civil, 1987.

[05] MathSoft, "MATHCAD 2000 User's Guide", MathSoft Inc. U.S, 2000.

[06] HAMBLY, E.C., Bridge Deck Behaviour, 2ª Edição, E & FN SPON, Londres e Nova Iorque, 1991.

[07] O'BRIEN, E.J., KEOGH, D.L., Bridge Deck Analysis, E & FN SPON, USA e Canada, 1999.

[08] NBR 7187 – Maio 1987 (ABNT, 1987), Projeto e Execução de Pontes de Concreto Armado e Protendido, Associação Brasileira de Normas Técnicas, Rio de Janeiro, 1987.

Figure 18 – Ultimate resisting moment for the internal members of section 1-1 for model 2